Biogeosciences
Discussions

Open Access

Rapid increasing trend of CO$_2$ and ocean acidification in the surface water of the Ulleung Basin, East/Japan Sea inferred from the observations from 1995 to 2004

J.-Y. Kim[1], D.-J. Kang[2], T. Lee[1], and K.-R. Kim[3]

[1]Department of Oceanography, Pusan National University, Busan 609-735, Korea
[2]Korea Institute of Ocean Science & Technology, Ansan 426-744, Korea
[3]School of Earth and Environment Sciences/Research Institute of Oceanography, Seoul National University, Seoul 151-747, Korea

Correspondence to: D.-J. Kang (djocean@kiost.ac)

Discussion Paper | Discussion Paper | Discussion Paper | Discussion Paper

BGD

10, 9573–9602, 2013

Rapid increasing trend of CO$_2$ and ocean acidification

J.-Y. Kim et al.

Title Page

Abstract	Introduction
Conclusions	References
Tables	Figures

|◄ | ►|
◄ | ►

Back | Close

Full Screen / Esc

Printer-friendly Version

Interactive Discussion

Abstract

Anthropogenic carbon is responsible for both global warming and ocean acidification. Efforts are underway to understand the role of ocean in a high CO_2 world on a global context. However, marginal seas received little attention despite their significant contribution to biogeochemical cycles. Here we report that the CO_2 increase and ocean acidification in the surface waters of the Ulleung Basin (UB) of the East/Japan Sea are much faster than the global mean, and possible causes are discussed. Twelve observations of surface $f\mathrm{CO_2}$ were made in the period from 1995 to 2004. The decadal trend of $f\mathrm{CO_2}$ increment was estimated by harmonic analysis. The estimated rates of increase of $f\mathrm{CO_2}$ were $1.97\,\mu\mathrm{atm\,yr^{-1}}$ for the atmosphere and $3.36\,\mu\mathrm{atm\,yr^{-1}}$ for the surface ocean. The rates exceed the global mean of $1.5\,\mu\mathrm{atm\,yr^{-1}}$. The ocean acidification trend, calculated from total alkalinity and $f\mathrm{CO_2}$, was estimated to be 0.04 pH units $\mathrm{decade^{-1}}$. Surface seawater of the UB has been acidified more rapidly compared to the global mean (0.02 pH units $\mathrm{decade^{-1}}$). Results show that, if warming strengthens the currents or advection in the marginal seas, biological pump will be enhanced. This would lead to compensation for the presumed reduction in oceanic uptake of atmospheric CO_2 in the warmer world, which warrants quantification worldwide.

1 Introduction

The IPCC (2007) announced that the anthropogenic CO_2 that has accumulated in the atmosphere since the Industrial Revolution is responsible for the enhanced greenhouse effect. The ocean is the ultimate mobile carbon storage reservoir in the Earth system. The surface ocean absorbs atmospheric CO_2 by means of both physical and biogeochemical processes. In the oceanic carbonate system, the dissolved carbon is transported to the deep ocean by the oceanic carbon pumps and eventually sequestrated in deep-sea sediments. Sabine et al. (2004) reported that about one-third of the CO_2 from the total anthropogenic CO_2 emissions is stored in the ocean. Despite the ocean's

Full Screen / Esc

Printer-friendly Version

Interactive Discussion

huge carbon storage capacity, atmospheric CO_2 is constantly increasing at an unprecedented rate; this disturbs the carbonate system in ways that will make air–sea exchange difficult in the high-CO_2 world of the future. Currently, results from established oceanic time-series stations show that the trend of increasing CO_2 in surface seawater exceeds that of the atmosphere (Bates, 2001; Keeling et al., 2004) and is accelerating ocean acidification (Caldeira and Wickett, 2003; Key et al., 2004; Orr et al., 2005).

Ocean carbon uptake is commonly described as a variety of carbon pumps, which operate by thermodynamics (e.g., temperature effects on the solubility of CO_2), physical transport (e.g., mixing and advection of water masses carrying various forms of carbon), sinking of soft-tissue (e.g., carbon uptake/release and export by phytoplankton during photosynthesis/respiration), and sinking of carbonate shells (e.g., formation and dissolution of $CaCO_3$) (Volk and Hoffert, 1985). These processes are easily affected, directly or indirectly, by temperature. The world ocean's temperature from the surface to 3000 m increased by 0.06 °C between the mid 1950s and mid 1990s because of an enhanced greenhouse effect (Levitus et al., 2005), and previous works have shown that the trend of increasing global sea surface temperature (SST) is about 0.08–0.14 °C decade^{-1} (Nicholls et al., 1996; Molinari et al., 1997; Casey and Cornillon, 2001). Soaring SST creates stronger stratification between the surface sea (upper mixed layer) and the deep ocean. It might affect the great ocean conveyor system by weakening deep water formation. The warming will also weaken the solubility pump and the biological carbon pump through fortified stratification. Overall, a positive feedback exists between global warming and ocean carbon uptake, thus making the situation worse.

Nearly all the ocean's dynamics can be observed and studied in the East/Japan Sea (EJS) despite its relatively small dimensions (Kim and Kim, 1996; Kim et al., 2001; Kang et al., 2003). The Ulleung Basin (UB), located on the western side of the southern EJS, has complex hydrography. The bifurcation of warm current entering through the Korea Strait leaves numerous spin-off mesoscale eddies at the surface, and beneath the surface, a number of cold currents originate from the winter overturning along the Siberian coast of the EJS. Winter mode water formation is occasionally observed (Kim

et al., 1991; Seung and Kim, 1993; Talley et al., 2003). The UB supports a high productivity ($> 220\,\mathrm{g\,C\,m^{-2}\,yr^{-1}}$) owing to its surface dynamics and coastal upwelling (Yamada et al., 2004; Yoo and Park, 2009). Because the UB has strong solubility pumps and biological pumps, it is an ideal laboratory for ocean carbon uptake studies. For this rea-
5 son some studies were carried out in the UB (Oh et al., 1999; Choi et al., 2011, 2012). In particular, it has been noted that the role of the coastal ocean in the global carbon budget has been underestimated (Wollast, 1998; Borges et al., 2005) and under debate (Cai and Dai, 2004; Thomas et al., 2004). Therefore, the role of the carbon pump in marginal seas should be reconsidered.
10   To reduce the scientific uncertainty in the prediction of future climate, a better understanding of the carbon flux among various reservoirs, especially the fluxes across the air–sea interface, is required. The Takahashi climatology (Takahashi et al., 2002) utilized all of the available data for modeling but still neglected marginal seas. Here, we like to emphasize the role of the marginal sea, as exemplified by the UB, and compare
15 it to that for the entire ocean. There is no time-series station comparable to BATS or HOT in the EJS. However, we attempted to fill the gap of oceanic CO_2 time series in the UB by interpolation using linear regression and harmonic function analysis of the data from repeated measurements. Although simplified and crude, an attempt to discern the long-term trend of CO_2 uptake and acidification in a marginal sea that operates its own
20 conveyor belt at a much faster time scale than the global ocean is here made for the first time.

2   Experimental methods and data analysis

2.1   Experimental methods

Measurements of the partial pressure of CO_2 (pCO_2) in the surface water and overly-
25 ing atmosphere, sea surface temperature (SST), and sea surface salinity (SSS) were carried out twelve times in the EJS from 1995 to 2004 (Table 1). The data that were

collected in the UB, the southwestern part of the EJS, were used in this study. The study area was defined as the region from 36–38° N latitude and 130–133° E longitude (Fig. 1).

The pCO$_2$ of surface seawater and the overlying atmosphere was measured by LiCor model 6252 non-dispersive infrared (NDIR) gas analyzer with a two-stage Weiss-type equilibrator. The CO$_2$ concentration from the NDIR was acquired every 2 s and, after statistical treatment for 1 min, averaged data were obtained and used as the final data. Three different standard gases were used to calibrate the NDIR. Every 12 h, a series of standard gases was analyzed for calibration; one of the standard gases was analyzed every 6 h to check for drift of the machine. Atmospheric and surface seawater pCO$_2$ were analyzed every 15 min and 45 min on the hour, respectively. Surface seawater pCO$_2$ was analyzed by equilibrating air with surface seawater fed to the equilibrator. In-situ SST and SSS were measured using thermosalinograph (SeaBird Electronics, Model SBE-21).

Total alkalinity (TA) was determined onboard by a potentiometric titration method using a closed cell (Millero et al., 1993). The TA data were obtained during cruises 9906, 0306, 0405, and 0410 (Table 1). Surface seawater pH values were obtained immediately after sampling by a spectrophotometric method using the indicator dye m-cresol purple (Clayton and Byrne, 1993). Determination of surface seawater pH values was carried out during cruises 9906, 0306, 0406, and 0410 (Table 1).

2.2 Air–sea flux estimation

The CO$_2$ flux (mmol C m^{-2} d^{-1}) was estimated from following equation;

$$\text{Flux} = k \times s \times \Delta f\text{CO}_2$$

where k is the gas transfer velocity (cm h^{-1}), s is the solubility of CO$_2$ gas in seawater (mol kg^{-1} atm^{-1}; Weiss, 1974), and ΔfCO$_2$ is the difference between atmospheric and surface seawater fCO$_2$. We choose the formulas for k and the wind speed relationships

Title Page

Abstract | Introduction

Conclusions | References

Tables | Figures

|◄ | ►|

◄ | ►

Back | Close

Full Screen / Esc

Printer-friendly Version

Interactive Discussion

used by Wanninkhof (1992). The NCEP wind speed data (http://www.esrl.noaa.gov/psd/data/reanalysis/) averaged on monthly scale in 36–38° N latitude and 130–133° E longitude was used to estimate for flux.

3 Results and discussion

3.1 General characteristics of $f\text{CO}_2$ and CO_2 flux in the UB

The secular variation of mean $f\text{CO}_2$ in the surface water and overlying atmosphere of the UB from 1995 to 2004 is shown in Fig. 2. The $f\text{CO}_2$ in the surface seawater ranged from 125 to 472 µatm with a mean value of 348.2 µatm (sd = 41.6), and the $f\text{CO}_2$ from the overlying atmosphere varied from 344 to 393 µatm with a mean value of 369 µatm (sd = 7.8). The $f\text{CO}_2$ in the surface water was lower than the $f\text{CO}_2$ in the atmosphere indicating that the surface seawater was undersaturated to atmospheric CO_2 in this area.

Generally, the secular trend of $f\text{CO}_2$ includes the long-term linear trend as well as the cyclic seasonal variation (Keeling et al., 2004). The long-term trend can be regarded as a linear increase with a constant rate. We determined trends of annual increase for both the $f\text{CO}_2^{\text{sea}}$ and the $f\text{CO}_2^{\text{air}}$ by applying a linear fit to the time-series data (Fig. 2). The slope of the regression result, which means annual increasing rate, for $f\text{CO}_2^{\text{sea}}$ was estimated to be 3.36 µatm yr^{-1} and that for the $f\text{CO}_2^{\text{air}}$ was 1.97 µatm yr^{-1}. It was assumed that $f\text{CO}_2$ had increased annually in the UB from 1995 through 2004 without any consideration about seasonal variability. To analyze seasonal data, the effect of the annual increase should be excluded. Hence, the data were normalized to the year 1995, when it was the initial time of observation.

The harmonic function, which is the sum of two components defined as the one-year and half-year component, has been used primarily to reconstruct time series data. Since this analysis method was first introduced by Nojiri et al. (1999), harmonic functions have been used extensively for $f\text{CO}_2$ variability studies (Zeng et al., 2002; Lüger

et al., 2004; Chierici et al., 2006). We applied the harmonic function analysis to $f\text{CO}_2$ data from the UB to estimate the decadal trend of CO_2 and to separate thermal and non-thermal effects on the $f\text{CO}_2$. Because harmonic function analysis is a technique for annual data, we used $f\text{CO}_2$ data that had been normalized to the reference year (1995) by assuming a constant annual increase rate (r_a) of $3.36\,\mu\text{atm}\,\text{yr}^{-1}$ for the surface seawater and $1.97\,\mu\text{atm}\,\text{yr}^{-1}$ for the atmosphere, respectively.

The $f\text{CO}_2$ was normalized to the year 1995 by using the following equation:

$$f\text{CO}_2^{1995} = f\text{CO}_2^{\text{in-situ}} - r_a \times (\text{Year} - 1995) \qquad (1)$$

where $f\text{CO}_2^{\text{in-situ}}$ is the measured data, r_a is the annual increasing rates in the surface seawater ($3.36\,\mu\text{atm}\,\text{yr}^{-1}$) and in the atmosphere ($1.97\,\mu\text{atm}\,\text{yr}^{-1}$), and Year is the year during which the data were collected.

We subsequently applied the following harmonic function to the normalized $f\text{CO}_2$:

$$f\text{CO}_2^{1995}(t) = C + C_1 \times \sin(2\pi t) + C_2 \times \cos(2\pi t) + C_3 \times \sin(4\pi t) + C_4 \times \cos(4\pi t) \qquad (2)$$

The set of five constant coefficients, C, C_1, C_2, C_3, and C_4, ensured a satisfactory fit of the harmonic function of Eq. (2) to the observed data ($R^2 = 0.82$ for seawater, $R^2 = 0.86$ for air), when the constant coefficients were equal to these values:

$C = 326.24$, $C_1 = -36.15$, $C_2 = 13.88$, $C_3 = 8.19$, $C_4 = 23.94$ (for seawater),
$C = 357.12$, $C_1 = 4.4$, $C_2 = 5.74$, $C_3 = -2.33$, $C_4 = -0.13$ (for air).

Monthly variations in $f\text{CO}_2^{1995}$ in the atmosphere and in the surface seawater which subtract the annual increaing trend by normalizing to the year of 1995 and the harmonic function analysis results are shown in Fig. 3.

Lastly, using Eq. (1), we recalculated $f\text{CO}_2^*$, which represents the $f\text{CO}_2$ with both the secular trend and the seasonal variation set to the reference year of 1995 as shown in the following:

$$f\text{CO}_2^* = f\text{CO}_2^{1995}(t) + r_a \times (\text{Year} - 1995) \qquad (3)$$

The regression of observed ($f\text{CO}_2$) and fitted values ($f\text{CO}_2^*$) appeared on Fig. 4 and yielded the following:

$$f\text{CO}_2^*(\text{sea}) = 0.87 \times f\text{CO}_2 + 41.76 \quad R^2 = 0.86, \quad n = 11 \qquad (4)$$

$$f\text{CO}_2^*(\text{air}) = 0.98 \times f\text{CO}_2 + 8.25 \quad R^2 = 0.94, \quad n = 10 \qquad (5)$$

The mean of the differences between $f\text{CO}_2$ and $f\text{CO}_2^*$ for the seawater and the atmosphere were 0.63 µatm and −0.15 µatm, respectively. The root mean square deviations were estimated 13.6 µatm (sea) and 2.5 µatm (air), which were smaller than the standard deviation derived from the spatiotemporal averaging data of the UB (41.6 µatm in $f\text{CO}_2^{\text{sea}}$ and 7.8 µatm in $f\text{CO}_2^{\text{air}}$).

The sea-air CO_2 fluxes in 1995 and 2004 were estimated in order to evaluate the effect of the last decadal increasing trend in $f\text{CO}_2$. The sea-air CO_2 fluxes were evaluated to be -0.95 ± 0.53 mol m^{-2} yr^{-1} for 1995 and -0.68 ± 0.49 mol m^{-2} yr^{-1} for 2004. This result shows that the UB acts as a carbon sink and its carbon sink efficiency in unit area is almost 1.6 (±0.3) − fold higher than global ocean (-0.51 mol m^{-2} yr^{-1}, Takahashi et al., 2002). However the flux had been decreased about 28 % during the last decade. Choi et al. (2012) and Oh et al. (1999) reported that the annual integrated CO_2 flux in this area was -2.47 ± 1.26 mol m^{-2} yr^{-1} and -2.2 mol m^{-2} yr^{-1}, which were larger than our results. The transiency of their observations could lead overestimation in CO_2 flux because of the complexity of the monthly variability and significant seasonal amplitude in $f\text{CO}_2^{\text{sea}}$ in the UB.

3.2 Seasonal variability and controlling factors of $f\text{CO}_2$ in the UB

The monthly variation in $f\text{CO}_2^{\text{sea}}$ and $f\text{CO}_2^{\text{air}}$ is shown in Fig. 3 and the $f\text{CO}_2^{\text{sea}}$ controlling parameters such as sea surface temperature (SST), mixed layer depth (MLD) based on the climatology data (de Boyer- Montégut et al., 2004), and chlorophyll a concentration inferred from the SeaWiFS data between 1998 and 2007 are represented in Fig. 5a–c. The SST reached a minimum in winter (February) and a maximum in sum-

mer (August and September) and had a mean value of 18.4 °C. The monthly variation in $f\mathrm{CO}_2^{\mathrm{air}}$ was opposite in phase to that of SST. The monthly variation pattern of $f\mathrm{CO}_2^{\mathrm{air}}$ followed the general seasonal cycle of $f\mathrm{CO}_2$ (or $p\mathrm{CO}_2$) monitored in the North Hemisphere; i.e., the $f\mathrm{CO}_2^{\mathrm{air}}$ reached its maximum value in spring and minimum value in summer. The $f\mathrm{CO}_2^{\mathrm{sea}}$, meanwhile, showed more complex variation than did the $f\mathrm{CO}_2^{\mathrm{air}}$. The monthly mean of the $f\mathrm{CO}_2^{\mathrm{sea}}$ in February, March, and April was lower than the average value (348.2 µatm) but that in August and December was above the average. The May–September data were close to the average. During the warm season (June and August), relatively high $f\mathrm{CO}_2^{\mathrm{sea}}$ was associated with elevated SST. During the fall and winter (October to February), monthly $f\mathrm{CO}_2^{\mathrm{sea}}$ values were higher than those in spring (April and May). This difference was a result of vertical entrainment of CO_2-rich subsurface water despite the decreasing SST. Deepening of MLD (> 50 m) supported high $f\mathrm{CO}_2^{\mathrm{sea}}$ phenomenon in winter (Fig. 5b). Comparison of the normalized total CO_2 (NTCO_2) in the EJS showed the difference of $\sim 100\,\mathrm{µmol\,kg^{-1}}$ in surface layer between summer and winter (Park, 1997). It also could be a result of the biological drawdown of CO_2 in March and April, when the $f\mathrm{CO}_2^{\mathrm{sea}}$ attained its lowest value. During March and April, satellite-based chlorophyll a concentration reached a peak value ($> 1\,\mathrm{mg\,m^{-3}}$) suggesting a possibility of biological CO_2 drawdown (Fig. 5c).

Takahashi et al. (2002) proposed a method for estimating the relative importance of the effects of biological activity and seasonal temperature change on the $p\mathrm{CO}_2$ of surface seawater. In order to estimate the relative magnitude of these effects, the ratio of the thermal effect (effect of temperature change) to the non-thermal effect (effect of biological activity and vertical mixing) was adapted after the method proposed by

Takahashi et al. (2002) as the following equations:

$$fCO_2^{therm} = \overline{fCO_2} \times \exp[0.0423 \cdot (SST - \overline{SST})] \tag{6}$$

$$fCO_2^{non\text{-}therm} = fCO_2 \times \exp[0.0423 \cdot (\overline{SST} - SST)] \tag{7}$$

$$\Delta fCO_2^{therm} = fCO_{2\,max}^{therm} - fCO_{2\,min}^{therm} \tag{8}$$

$$\Delta fCO_2^{non\text{-}therm} = fCO_{2\,max}^{non\text{-}therm} - fCO_{2\,min}^{non\text{-}therm} \tag{9}$$

where SST is the surface seawater temperature in °C, and the $\overline{fCO_2}$ and $\overline{SST}$ refer to the annual average of observed fCO_2 and SST values, respectively.

The dependence of fCO_2 variability in the UB on the thermal (fCO_2^{therm}) and non-thermal ($fCO_2^{non\text{-}therm}$) effects was separated by the equations above (Eqs. 6 and 7). The results are shown in Fig. 5d and e. The fCO_2^{therm} followed the same pattern as the seasonal SST variation (Fig. 5d and a). The peak-to-peak amplitudes of the seasonal cycles of SST and fCO_2^{therm} (ΔfCO_2^{therm}, Eq. 8) were $\sim 17\,°C$ and 236 µatm, respectively, which means that an 1 °C temperature change makes a 14 µatm change in fCO_2. Takahashi et al. (1993) suggested the thermodynamic relationship between pCO_2 and temperature $((\partial pCO_2/\partial T)/pCO_2 = 0.0423\,°C^{-1})$, our data showed almost close to it ($0.0376\,°C^{-1}$). However, the ΔfCO_2^{therm} was larger than that observed at Station "P" (100 µatm, Wong and Chan, 1991) and at BATS (150 µatm, Bates, 2001), which located at the comparable latitude as the UB. Larger seasonal variation of SST (> 17 °C) may have caused such a difference.

On the other hand, $fCO_2^{non\text{-}therm}$ reached its highest value during the cold season and its lowest value during the warm season. The peak-to-peak amplitude was 193 µatm, which was smaller than the value from the Ross Sea (260 µatm, Sweeney, 2000) but much larger than the value from BATS (115 µatm, Bates, 2001). This high $fCO_2^{non\text{-}therm}$ value in winter was due to (1) relatively low biological carbon uptake during the cold season, and (2) stronger vertical mixing that pumps up high-CO_2 subsurface water. The decrease in the $fCO_2^{non\text{-}therm}$ value of more than 100 µatm in spring was attributed

Full Screen / Esc

Printer-friendly Version

Interactive Discussion

to carbon fixation by the spring bloom (Fig. 5e and c). In summer, the value decreased because of weakening of vertical mixing caused by stratification (Fig. 5b and e).

The seasonal variation in $f\text{CO}_2$ can be explained by the sum of the thermal and non-thermal effects. The ratio between the thermal effect and the non-thermal effect was estimated to be almost equal to one ($\Delta f\text{CO}_2^{\text{therm}}/\Delta f\text{CO}_2^{\text{non-therm}} = 1.2$) in the UB, which suggested that the thermal effect was almost balanced with the non-thermal effect. A similar result (0.9) was obtained at Station "P" in the eastern subarctic Pacific Ocean (50° N, 145° W) during the period 1973–1978 (Wong and Chan, 1991). On the other hand, the ratio differed significantly from that found for the BATS (2.7) (Bates, 2001) or the Ross Sea (0.02) (Sweeney, 2000) values (Table 2).

In summary, the contribution of temperature variation to the seasonality of $f\text{CO}_2$ was almost equivalent to the non-thermal effect. However, the relative contribution varied with the season (Fig. 5f). Non-thermal effect contributed to the surface $f\text{CO}_2$ drawdown in summer, while the surface $f\text{CO}_2$ elevation in winter. According to Sarmiento and Gruber (2006), $p\text{CO}_2$ in the North Pacific is not affected by one dominant factor among SST, biological activity, and vertical mixing but is affected by their combined effect. Their explanation about the controlling factors of $p\text{CO}_2$ in the North Pacific could be applied to similar features of the $f\text{CO}_2$ in the UB.

3.3 Decadal trend of $f\text{CO}_2$ in the UB

Decadal trend of the modeled $f\text{CO}_2$ (i.e., $f\text{CO}_2^*$) based on the combination of a linear increasing trend and a harmonic function analysis using observed data from the UB is shown in Fig. 6. The long-term atmospheric $p\text{CO}_2$ variation observed at Gosan (33°17.4′ N, 126°9.9′ E), Jeju Island, Korea (Cho et al., 2005) is also shown in the figure for comparison with $f\text{CO}_2^{\text{air}}$ measured in the UB (Fig. 6a).

The $f\text{CO}_2^{\text{air}}$ in the UB coincided with $p\text{CO}_2^{\text{air}}$ at Gosan owing to the shorter turnover time of atmospheric CO_2 than that in the ocean. The trends of increasing $p\text{CO}_2$ at Gosan and $f\text{CO}_2$ in the UB were $1.9\,\text{ppm}\,v\,\text{yr}^{-1}$ and $1.97\,\mu\text{atm}\,\text{yr}^{-1}$, respectively. These

values were slightly larger than the global mean $1.5\,\mathrm{ppm}\,v\,\mathrm{yr}^{-1}$ (IPCC, 2007). Still larger was the decadal increase trend of $f\mathrm{CO_2}$ observed in the UB. The $f\mathrm{CO_2^{sea}}$ in the UB had been increasing gradually at a rate of $3.36\,\mathrm{\mu atm}\,\mathrm{yr}^{-1}$, which was almost similar to result measured from Station ALOHA ($22°45'$ N, $158°$ W) of the HOT between 1997 and 2004 ($3.2\,\mathrm{\mu atm}\,\mathrm{yr}^{-1}$; Keeling et al., 2004). However, when we compared the peak-to-peak amplitudes of the $f\mathrm{CO_2^{sea}}$ in the UB with those at station ALOHA, we found that the UB exhibits a stronger seasonality ($99.5\,\mathrm{\mu atm}$) than did station ALOHA ($40\,\mathrm{\mu atm}$).

Since the work of Inoue et al. (1995), numerous studies have focused on the rate of $\mathrm{CO_2}$ increase based on monitoring and survey data. For the sake of comparing the decadal trend of the $f\mathrm{CO_2}$ in the UB with other regions, previously published data covering approximately 30 different oceanic areas are listed in Table 3. Rates of increase of $f\mathrm{CO_2}$ are plotted as a function of the latitude in Fig. 7. Generally, the increasing rate in most areas is close to the global average ($1.5\,\mathrm{\mu atm}\,\mathrm{yr}^{-1}$; IPCC 2007), but the rate in the middle latitudes of the Northern Hemisphere is higher. We could infer from this result that human activities might influence the rate of increase of $\mathrm{CO_2}$ in surface seawater.

3.4 Acidification rate

As surface water $\mathrm{CO_2}$ has been increasing, the pH of the surface seawater has been decreasing, an effect called ocean acidification. The decadal trend of pH in the UB was estimated based on total alkalinity (TA) data from this study and $f\mathrm{CO_2^*}$. The pH values were calculated from TA and simulated $f\mathrm{CO_2^*}$ by CO2SYS (Lewis and Wallace, 1998). The carbonate dissociation constants (K_1 and K_2) used in these calculations was those of Mehrbach et al. (1973) as refit by Dickson and Millero (1987). We assumed the TA of surface seawater to be constant at $2266 \pm 17\,\mathrm{\mu eq}\,\mathrm{kg}^{-1}$, the average value of 60 measurements during the study period, because the seasonality and secular trends were not significant. These calculated pH values were in good agreement with the measured ones ($R^2 = 0.8$).

As the surface fCO$_2$ increased, the pH value in the surface seawater of the UB, while fluctuating seasonally, decreased at the rate of 0.04 pH units decade^{-1} since 1995 (Fig. 8). The pH in the surface ocean decreased by 0.1 pH units between 1750 and 1994, which was noted as an unprecedented decline by Sabine et al. (2004). To compare fCO$_2$ increasing trend and pH decreasing trend in the UB with global trend, we also plotted time series of fCO$_2$ and pH from Station ALOHA data. Since 1988, the pCO$_2$ at Station ALOHA has increased at a rate of $\sim 2\,\mu$atm yr^{-1} and mixed layer pH has declined by 0.02 pH units per decade (Fig. 8, Doney et al., 2012). IPCC (2007) reported that the rate of decrease of pH was estimated at about 0.02 pH units decade^{-1} based on station data at HOT, BATS, and ESTOC since 1980. Compared with the global trend, surface seawater of the UB was being acidified almost twice as rapidly.

Under the assumption of constant TA and surface seawater temperature, 10 % increase of fCO$_2$ (i.e. 33.6 μatm increase in a decade) may reduce pH by 0.036 pH units. A seawater temperature rise of 1 °C may also decrease pH by 0.01 pH units at a pressure of 1 atm (Gieskes, 1969). The sea surface temperature in the EJS increased by 0.2–0.7 °C during the last decade (Kim et al., 2007; Yeh et al., 2010), which is a much faster warming than the global average (0.13 °C decade^{-1}; Rayner et al., 2006). This warming contributed to a pH decrease of 0.002–0.007 pH units which was equivalent to 5–20 % of the pH decline in the UB during the last decade. Therfore, the ocean acidification in the UB was mainly driven by the fCO$_2$ increase (~ 90 %), while the warming effect was relatively small (about 5–20 %).

References

Bates, N.: Interannual variability of oceanic CO_2 and biogeochemical properties in the Western North Atlantic subtropical gyre, Deep-Sea Res. Pt. II, 48, 1507–1528, 2001.

Bates, N.: Interannual variability of the oceanic CO_2 sink in the subtropical gyre of the North Atlantic Ocean over the last 2 decades, J. Geophys. Res., 112, C09013, doi:10.1029/2006JC003759, 2007.

Borges, A. V., Delille, B., and Frankignoulle, M.: Budgeting sinks and sources of CO_2 in the coastal ocean: diversity of ecosystems counts, Geophys. Res. Lett., 32, L14601, doi:10.1029/2005GL023053, 2005.

Cai, W.-J. and Dai, M.: Comment on "Enhanced Open Ocean Storage of CO_2 from Shelf Sea Pumping", Science, 306, 1477, doi:10.1126/science.1102132, 2004.

Caldeira, K. and Wickett, M. E.: Anthropogenic carbon and ocean pH, Nature, 425, doi:10.1038/425365a, 2003.

Casey, K. S. and Cornillon, P.: Global and regional sea surface temperature trends, J. Climate, 14, 3801–3818, 2001.

Chierici, M., Fransson, A., and Nojiri, Y.: Biogeochemical processes as drivers of surface $f\,CO_2$ in contrasting provinces in the subarctic North Pacific Ocean, Global Biogeochem. Cy., 20, GB1009, doi:10.1029/2004GB002356, 2006.

Cho, C., Oh, S.-N., Park, K.-J., Choi, B.-C., Park, M.- K., and Kim, K.-R.: The distribution characteristics of atmospheric CO_2 in the Korean Peninsula and the expectations on its annual growth trend by the year 2015, Asia-Pac. J. Atmos. Sci., 41, 371–385, 2005.

Choi, S. H., Kim, D., Shim, J. H., and Min, H. S.: The spatial distribution of surface $f\,CO_2$ in the Southwestern East Sea/Japan Sea during summer 2005, Ocean. Sci. J., 46, 13–21, 2011.

Choi, S. H., Kim, D., Shim, J. H., Kim, K.-H., and Min, H. S.: Seasonal variations of surface $f\,CO_2$ and sea-air fluxes in the Ulleung Basin of the East/Japan Sea, Terr. Atmos. Ocean. Sci., 23, 343–353, 2012.

Clayton, T. D. and Byrne, R. H.: Spectrophotometric seawater pH measurements: total hydrogen ion concentration scale calibration of m-cresol purple and at sea results, Deep-Sea Res., 40, 2115–2129, 1993.

Corbiere, A., Metzl, N., Reverdin, G., Brunet, C., and Takahashi, T.: Interannaul and decadal variability of the oceanic carbon sink in the North Atlantic subpolar gyre, Tellus B, 59, 168–178, 2007.

de Boyer-Montégut, C., Madec, G., Fisher, A. S., Lazar, A., and Iudicone, D.: Mixed layer depth over the global ocean: an examination of profile data and a profile-based climatology, J. Geophys. Res., 109, C12003, doi:10.1029/2004JC002378, 2004.

Dickson, A. G. and Millero, F. J.: A comparison of the equilibrium constants for the dissociation of carbonic acid in seawater media, Deep-Sea Res., 34, 1733–1743, 1987.

Doney, S., Fabry, V. J., Feely, R. A., and Kleypas, J. A.: Ocean acidification: the other CO_2 problem, Ann. Rev. Mar. Sci., 1, 169–192, 2009.

Doney, S., Ruckelshaus, M., Duffy, E., Barry, J., Chan, F., English, C., Galindo, H., Grebmeier, J., Hollowed, A., Knowlton, N., Polovina, J., Rabalais, N., Sydeman, W., and Talley, L.: Climate change impacts on marine ecosystems, Ann. Rev. Mar. Sci., 4, 1–27, 2012.

Dore, J. E., Lukas, R., Sadler, D. W., and Karl, D. M.: Climate driven changes to the atmospheric CO_2 sink in the subtropical North Pacific Ocean, Nature, 424, 754–757, 2003.

Gieskes, J. M.: Effect of temperature on the pH of seawater, Limnol. Oceanogr., 14, 679–685, 1969.

Inoue, H. Y. and Ishii, M.: Variations and trends of CO_2 in the surface seawater in the Southern Ocean south of Australia between 1969 and 2002, Tellus B, 57, 58–69, 2005.

Inoue, H. Y., Matsueda, H., Ishii, M., Fushimi, K., Hirota, M., Asanuma, I., and Takasugi, Y.: Long-term trend of the partial pressure of carbon dioxide (pCO_2) in surface waters of the western North Pacific, 1984–1993, Tellus B, 47, 391–413, 1995.

Intergovernmental Panel on Climate Change (IPCC): Climate change 2007: The physical science basis, Cambridge University Press, 996 pp., 2007.

Ishii, M., Saito, S., Nemoto, K., Midorikawa, T., and Inoue, H.: Decadal variability of the oceanic CO_2 in the western Equatorial Pacific warm pool, in: Understanding North Pacific Carbon-cycle Changes: a Data Synthesis and Modeling Workshop, Seattle, 2004.

Kang, D.-J., Park, S., Kim, Y.-G., Kim, K., and Kim, K.-R.: A Moving-Boundary Box Model (MBBM) for oceans in change: an application to the East/Japan Sea, Geophys. Res. Lett., 30, 1299, doi:10.1029/2002GL016486, 2003.

Keeling, C. D., Brix, H., and Gruber, N.: Seasonal and long-term dynamics of the upper ocean carbon cycle at Station ALOHA near Hawaii, Global Biogeochem. Cy., 18, GB4006, doi:10.1029/2004GB002227, 2004.

Key, R. M., Kozyr, A., Sabine, C. L., Lee, K., Wanninkhof, R., Bullister, J., Feely, R. A., Millero, F., Mordy, C., and Peng, T.-H.: A global ocean carbon climatology: Results from GLODAP, Global Biogeochem. Cy., 18, GB4031, doi:10.1029/2004GB002247, 2004.

Title Page

Abstract | Introduction

Conclusions | References

Tables | Figures

◄ | ►

◄ | ►

Back | Close

Full Screen / Esc

Printer-friendly Version

Interactive Discussion

Kim, K., Kim, K.-R., Chung, J. Y., Yoo, H. S., and Park, S. G.: Characteristics of physical properties in the Ulleung Basin, J. Korean Soc. Oceanogr., 26, 83–100, 1991.

Kim, K., Kim, K.-R., Min, D., Volkov, Y., Yoon, J.-H., and Takematsu, M.: Warming and structural changes in the East Sea (Japan Sea): a clue to the future changes in global oceans?, Geophys. Res. Lett., 28, 3293–3296, 2001.

Kim, K.-R. and Kim, K.: What is happening in the East Sea (Japan Sea)?: recent chemical observation during CREAMS 93–96, J. Korean Soc. Oceanogr., 31, 164–172, 1996.

Kim, S., Zhang, C.-I., Kim, J.-Y., Oh, J.-H., Kang, S., and Lee, J. B.: Climate variability and its effects on major fisheries in Korea, Ocean Sci. J., 42, 179–192, 2007.

Lefévre, N., Watson, A. J., Olsen, A., Rios, A. F., and Pérez, F. F.: A decrease in the sink for atmospheric CO_2 in the North Atlantic, Geophys. Res. Lett., 31, L07306, doi:10.1029/2003GL018957, 2004.

Lewis, E. and Wallace, D. W. R.: CO2SYS-Program developed for the CO_2 system calculations. Carbon Dioxide Information Analysis Center, Oak Ridge, 31 pp., 1998.

Levitus, S., Antonov, J., and Boyer, T.: Warming of the world ocean, 1955–2003, Geophys. Res. Lett., 32, L02604, doi:10.1029/2004GL021592, 2005.

Lüger, H., Wallace, D. W. R., Körtzinger, A., and Nojiri, Y.: The pCO_2 variability in the midlatitude North Atlantic Ocean during a full annual cycle, Global Biogeochem. Cy., 18, GB3023, doi:10.1029/2003GB002200, 2004.

Lüger, H., Wanninkhof, R., Wallace, D. W. R., and Körtzinger, A.: CO_2 fluxes in the subtropical and subarctic North Atlantic based on measurements from a volunteer observing ship, J. Geophys. Res., 111, C06024, doi:10.1029/2005JC003101, 2006.

Mehrbach, C., Culberson, C. H., Hawley, J. E., and Pytkowicz, R. M.: Measurement of the apparent dissociation constants of carbonic acid in seawater at atmospheric pressure, Limnol. Oceanogr., 18, 897–907, 1973.

Millero, F. J., Zhang, J.-Z., Lee, K., and Campbell, D. M.: Titration alkalinity of seawater, Mar. Chem., 44, 153–165, 1993.

Molinari, R. L., Mayer, D. A., Fester, J. F., and Bezdek, H. F.: Multiyear variability in the near-surface temperature structure of the midlatitude western North Atlantic Ocean, J. Geophys. Res., 102, 3267–3278, 1997.

Nicholls, N., Grusz, V. V., Jouzel, J., Karl, T., Ogallo, L., and Parker, D.: Observed climate variability and change, in: Climate Change 1995: The Science of Climate Change, edited by: Houghton, J. and IPCC, Cambridge University Press, 133–192, 1996.

Nojiri, Y. and Tsumori, H.: Ocean carbon source and sinks regional view: North Pacific: data analysis of 12 years of monthly observation by the 3 VOS, in: Changing Times: An International Ocean Biogeochemical Time-Series Workshop, IOC/UNESCO, Paris, France, 2007.

Nojiri, Y., Fujinuma, Y., Zeng, J., and Wong, C. S.: Monitoring of pCO$_2$ with complete seasonal coverage utilizing a cargo ship M/S *Skaugran* between Japan and Canada/US, in: Proceedings of the Second International Symposium of CO$_2$ in the Oceans, Tsukuba, Japan, 17–23, 1999.

Oh, D. C.: A study on the characteristics of fCO$_2$ distributions and CO$_2$ flux at the air–sea interface in the seas around Korea, M.S. thesis, Seoul National University, 1998.

Oh, D.-C., Park, M.-K., Choi, S.-H., Kang, D.-J., Park, S. Y., Hwang, J. S., Andreev, A., Hong, G. H., and Kim, K.-R.: The air–sea exchange of CO$_2$ in the East Sea (Japan Sea), J. Oceanogr., 55, 157–169, 1999.

Omar, A. M. and Olsen, A.: Reconstructing the time history of the air–sea CO$_2$ disequilibrium and its rate of change in the eastern subpolar North Atlantic, 1972–1989, Geophys. Res. Lett., 33, L04602, doi:10.1029/2005GL025425, 2006.

Orr, J. C., Fabry, V. J., Aumont, O., Bopp, L., Doney, S. C., Feely, R. A., Ganadesikan, A., Gruber, N., Ishida, A., Joos, F., Key, R. M., Lindsay, K., Maier-Reimer, E., Matear, R., Monfray, P., Mouchet, A., Najjar, R. G., Plattner, G.-K., Rodgers, K. B., Sabine, C. L., Sarmiento, J. L., Schlitzer, R., Slater, R. D., Totterdell, I. J., Weirig, M.-F., Yamanaka, Y., and Yool, A.: Anthropogenic ocean acidification over the twenty-first century and its impact on calcifying organisms, Nature, 437, 681–686, 2005.

Park, S. Y.: A study on the carbon cycle in the deep waters of the East Sea, M.S. thesis, Seoul National University, 1997.

Rayner, N. A., Brohan, P., Parker, D. E., Folland, C. K., Kennedy, J. J., Vanicek, M., Ansell, T. J., and Tett, S. F. B.: Improved analyses of changes and uncertainties in sea surface temperature measured in situ since the mid-nineteenth century: the HadSST2 dataset, J. Climate, 19, 446–469, 2006.

Sabine, C. L., Feely, R. A., Gruber, N., Key, R. M., Lee, K., Bullister, J. L., and Wanninkhof, R.: The ocean sink for anthropogenic CO$_2$, Science, 305, 367–371, 2004.

Santana-Casiano, J. M., González-Dávila, M., Rueda, M.-J., Llinás, O., and González-Dávila, E.-F.: The interannual variability of oceanic CO$_2$ parameters in the northeast Atlantic subtropical gyre at the ESTOC site, Global Biogeochem. Cy., 21, GB1015, doi:10.1029/2006GB002788, 2007.

Title Page

Abstract | Introduction

Conclusions | References

Tables | Figures

|◄ | ►|

◄ | ►

Back | Close

Full Screen / Esc

Printer-friendly Version

Interactive Discussion

Sarmiento, J. L. and Gruber, N.: Ocean biogeochemical dynamics, Princeton Univ. Press, 2006.

Schuster, U. and Watson, A. J.: A variable and decreasing sink for atmospheric CO_2 in the North Atlantic, J. Geophys. Res., 112, C11006, doi:10.1029/2006JC003941, 2007.

Seung, Y. H. and Kim, K.: A numerical modeling of the East Sea circulation, J. Korean Soc. Oceanogr., 28, 292–304, 1993.

Sweeney, C.: Biogeochemical regimes and meso-scale variability in the Ross Sea, Antarctica, Ph.D. Thesis, Columbia University, 2000.

Takahashi, T., Olafsson, J., Goddard, J., Chipman, D. W., and Sutherland, S. C.: Seasonal variation of CO_2 and nutrients in the high-latitude surface oceans: a comparative study, Global Biogeochem. Cy., 7, 843–878, 1993.

Takahashi, T., Sutherland, S. C., Sweeney, C., Poisson, A., Metzl, N., Tilbrook, B., Bates, N., Wanninkhof, R., Feely, R. A., Sabine, C., Olafsson, J., and Nojiri, Y.: Global sea–air CO_2 flux based on climatological surface ocean pCO_2, and seasonal biological and temperature effects, Deep-Sea Res. Pt. II, 49, 1601–1622, 2002.

Takahashi, T., Sutherland, S. C., Feely, R. A., and Cosca, C. E.: Decadal variation of the surface water pCO_2 in the western and central equatorial Pacific, Science, 203, 852–856, 2003.

Takahashi, T., Sutherland, S. C., Feely, R. A., and Wanninkhof, R.: Decadal change of the surface water pCO_2 in the North Pacific: a synthesis of 35 years of observations, J. Geophys. Res., 111, C07S05, doi:10.1029/2005JC003074, 2006.

Talley, L. D., Lovanov, V., Ponomarev, V., Salyuk, A., Tishchenko, P., Zhabin, I., and Riser, S.: Deep convection and brine rejection in the Japan Sea, Geophys. Res. Lett., 30, 1159, doi:10.1029/2002GL016451, 2003.

Thomas, H., Bozec, Y., Elkalay, K., and de Baar, H. J. W.: Enhanced open ocean storage of CO_2 from shelf sea pumping, Science, 304, 1005–1008, 2004.

Tseng, C.-M., Wong, G. T. F., Chou, W.-C., Lee, B.-S., Sheu, D.-D., and Liu, K.-K.: Temporal variations in the carbonate system in the upper layer at the SEATS station, Deep-Sea Res. Pt. II, 54, 1448–1468, 2007.

Volk, T. and Hoffert, M. I.: Ocean carbon pumps: analysis of relative strengths and efficiencies in ocean-driven atmospheric CO_2 changes, in: The Carbon Cycle and Atmospheric CO_2: Natural Variations Archean to Present, edited by: Sundquist, E. T. and Broecker, W. S., Geophysical Monograph 32, American Geophysical Union, Washington, DC, 99–110, 1985.

Wanninkhof, R.: Relationship between wind speed and gas exchange over the ocean, J. Geophys. Res., 97, 7373–7382, 1992.

Watai, T., Kikuchi, M., and Nakazawa, T.: Temporal variations of surface oceanic and atmospheric CO_2 fugacity and total dissolved inorganic carbon in the northwestern North Pacific, J. Oceanogr., 54, 323–336, 1998.

Weiss, R. F.: Carbon dioxide in water and seawater: the solubility of a non-ideal gas, Mar. Chem., 2, 203–205, 1974.

Wollast, R.: Evaluation and comparison of the global carbon cycle in the coastal zone and in the open ocean, in: The Global Coastal Ocean, edited by: Brink, K. H. and Robinson, A. R., John Wiley & Sons, New York, 213–252, 1998.

Wong, C. S. and Chan, Y.-H.: Temporal variations in the partial pressure and flux of CO_2 at ocean station P in the subarctic northeast Pacific Ocean, Tellus B, 43, 206–223, 1991.

Yamada, K., Ishizaka, J., Yoo, S., Kim, H. C., and Chiba, S.: Seasonal and interannual variability of sea surface chlorophyll *a* concentration in the Japan/East (JES), Prog. Oceanogr. 61, 193–211, 2004.

Yeh, S.-W., Park, Y.-G., Min, H., Choi, C.-H., and Lee. J.-H.: Analysis of characteristics in the sea surface temperature variability in the East/Japan Sea, Prog. Oceanogr., 85, 213–223, 2010.

Yoo, S. and Park, J.: Why is the southwest the most productive region of the East Sea/Sea of Japan?, J. Marine Syst., 78, 301–315, 2009.

Zeng, J., Nojiri, Y., Murphy, P. P., Wong, C. S., and Fujinuma, Y.: A comparison of pCO_2 distributions in the northern North Pacific using results from a commercial vessel in 1995–1999, Deep-Sea Res. Pt. II, 49, 5303–5315, 2002.

Discussion Paper | Discussion Paper | Discussion Paper | Discussion Paper

BGD

10, 9573–9602, 2013

Rapid increasing trend of CO$_2$ and ocean acidification

J.-Y. Kim et al.

Title Page

Abstract | Introduction

Conclusions | References

Tables | Figures

◀ | ▶

◀ | ▶

Back | Close

Full Screen / Esc

Printer-friendly Version

Interactive Discussion

Table 1. Summary of cruise information and data for this study. SST, $f\mathrm{CO}_2^{\mathrm{air}}$, $f\mathrm{CO}_2^{\mathrm{sea}}$, $\Delta f\mathrm{CO}_2$, total alkalinity (TA), and pH are reported as averages with one standard deviations. The number of data is given in parentheses.

Cruise Name	Observation Period	Research Vessel	SST (°C)	$f\mathrm{CO}_2^{\mathrm{air}}$ (µatm)	$f\mathrm{CO}_2^{\mathrm{sea}}$ (µatm)	$\Delta f\mathrm{CO}_2$ (µatm)	TA (µeq kg^{-1})	pH	Source
9508	6 Aug–7 Aug 1995	R/V *Professor Khromov*	24.1 ± 1.5 (40)	352.6 ± 3.1 (40)	365.4 ± 13.6 (40)	12.4 ± 12.8 (40)	N/A	N/A	Oh et al. (1999)
9602	23 Feb–24 Feb 1996	R/V *Parvel Gordienko*	9.2 ± 1.2 (256)	362.9 ± 0.4 (256)	311.2 ± 14.3 (256)	−51.7 ± 14.4 (256)	N/A	N/A	Oh et al. (1999)
9607	31 Jul–10 Aug 1996	R/V *Professor Khromov*	25.6 ± 1.0 (233)	346.8 ± 2.6 (233)	359.7 ± 36.3 (233)	12.9 ± 35.7 (233)	N/A	N/A	Oh et al. (1999)
9703	19 Mar–7 Apr 1997	R/V *Parvel Gordienko*	12.5 ± 1.1 (463)	364.9 ± 3.2 (463)	266.5 ± 12 (463)	−98.4 ± 12.8 (463)	N/A	N/A	Oh (1998)
9906	25 Jun–1 Jul 1999	R/V *Roger Revelle*	20.9 ± 0.5 (669)	N/A	335.9 ± 10.5 (178)	N/A	2271 ± 10 (23)	8.04 ± 0.02 (23)	This study
0204	12 Apr–19 Apr 2002	R/V *Gargarinsky*	12.8 ± 1.4 (3857)	375.9 ± 8.6 (712)	280.5 ± 41.1 (1141)	−92.8 ± 41.2 (1142)	N/A	N/A	This study
0306	9 Jun–14 Jun 2003	R/V *Tamgu-5*	19.5 ± 0.4 (2233)	366.9 ± 2.3 (2233)	353.7 ± 19.2 (1319)	−29.1 ± 18.6 (1319)	2256 ± 21 (21)	8.06 ± 0.03 (29)	This study
0312	12 Dec–22 Dec 2003	R/V *Tamgu-5*	16.4 ± 0.5 (1392)	379.7 ± 0.9 (120)	390.1 ± 15.3 (401)	−3.9 ± 14.7 (401)	N/A	N/A	This study
0405	6 May–19 May 2004	R/V *Akademik Labrantiev*	17.8 ± 1.8 (5153)	376.6 ± 3.3 (846)	354 ± 23.6 (3113)	−50.1 ± 22.7 (3113)	2281 ± 8 (8)	N/A	This study
0406	10 Jun–11 Jun 2004	R/V *Tamgu-5*	19.8 ± 0.2 (334)	368.6 ± 0.3 (334)	336.5 ± 7 (194)	−50.7 ± 6.1 (194)	N/A	8.05 ± 0.02 (21)	This study
0409	14 Sep–15 Sep 2004	R/V *Tamgu-1*	26.2 ± 2.4 (806)	368.8 ± 3.9 (806)	348.8 ± 7.9 (245)	−26.6 ± 8.4 (245)	N/A	N/A	This study
0410	5 Oct–29 Oct 2004	R/V *Tamgu-5*	23.0 ± 1.2 (4362)	371.5 ± 2.9 (563)	379.3 ± 17.9 (2673)	−30.6 ± 16.4 (2673)	2261 ± 8 (8)	8.07 ± 0.03 (8)	This study

Table 2. Comparison of the contribution of thermal and non-thermal effects on the fCO$_2$ of surface seawater in various regions.

Station	Thermal effect (µatm)	Non-thermal effect (µatm)	Ratio (Therm/non-Therm)	Location	References
UB	236	193	1.2	36–38° N, 130–133° E	This Study
BATS	150	55	2.7	32°50′ N, 64°10′ W	Bates (2001), Takahashi et al. (2002)
Ross Sea	5	260	0.02	76°30′ S, 169° E–177° W	Sweeney (2000), Takahashi et al. (2002)
Station "P"	100	115	0.9	50° N, 145° W	Wong and Chan (1991), Takahashi et al. (2002)

Table 3. Rate of increase of surface seawater CO_2 at various regions of the world ocean.

Region	Increasing Rate ($\mu atm\,yr^{-1}$)	Duration	Area	Reference
North Pacific	1.3 ± 0.2	1970–2004	Whole Pacific	Takahashi et al. (2006)
Central Equatorial Pacific	1.8 ± 0.7	1979–2001	5° N–5° S	Takahashi et al. (2003)
Western Equatorial Pacific[a]	3.4 ± 0.4	1979–2001	5° N–5° S	Takahashi et al. (2003)
Western Equatorial Pacific[b]	1.2 ± 0.7		10° S–10° N, 150° E–160° W	Ishii et al. (2004)
Western North Pacific[a]	1.8 ± 0.6	1984–1993	15° N–35° N, 132° E–142° E	Inoue et al. (1995)
Western North Pacific[b]	0.5 ± 0.7	1984–1993	3° N–14° N, 132° E–142° E	Inoue et al. (1995)
Western North Pacific[c]	2.1	1995–2007	35° N, 147.5° E	Nojiri and Tsumori (2007)
Northwestern North Pacific	3.7	1992–1996	37.3° N, 141.47° E	Watai et al. (1998)
Central North Pacific	0.8	1995–2006	40° N, 175° E	Nojiri and Tsumori (2007)
Eastern North Pacific	0.9		35° N, 140° W	Nojiri and Tsumori (2007)
Western Subarctic North Pacific	0.6		45° N, 155° E	Nojiri and Tsumori (2007)
Eastern Subarctic North Pacific	1.7		54.5° N, 165° W	Nojiri and Tsumori (2007)
Station "P"	1.4		50° N, 145° W	Nojiri and Tsumori (2007)
North Atlantic gyre	4.4	1994–2005	22° N–50° N, 5° W–70° W	Schuster and Watson (2007)
Eastern North Atlantic	3.6	1995–2002	36° N–52° N, 10° W–35° W	Lüger et al. (2004, 2006)
Western North Atlantic	1.7	1995–2002	36° N–52° N, 36° W–70° W	Lüger et al. (2004, 2006)
North Atlantic Subpolar Gyre	1.8	1982–1998	50° N–70° N, 80° W–10° W	Lefévre et al. (2004)
Eastern Subpolar North Atlantic	3.0	1970s–1980s	50° N–64° N, 32° W–10° W	Omar and Olsen (2006)
Western Subpolar North Atlantic	3.0	1994–2003	53° N–62° N, 20° W–45° W	Corbiere et al. (2007)
South Indian Ocean[a]	1.1		20° S	Inoue and Ishii (2005)
South Indian Ocean[b]	1.4		40° S	Inoue and Ishii (2005)
South of Australia (Sub-Antarctic Zone)	1		50° S, 140° E–160° E	Inoue and Ishii (2005)
South of Australia (Polar Frontal Zone)	1.5		55° S, 140° E–160° E	Inoue and Ishii (2005)
South of Australia (Polar Zone)	1.8		58° S, 140° E–160° E	Inoue and Ishii (2005)
ALOHA[a]	2.5 ± 0.3	1989–2001	22.7° N, 158° W	Dore et al. (2003)
ALOHA[b]	3.2 ± 0.4	1997–2002	22.7° N, 158° W	Keeling et al. (2004)
ALOHA[c]	1.4 ± 0.2	1988–1996	22.7° N, 158° W	Keeling et al. (2004)
SEATS	4.2 ± 3.2	1995–2004	18° N, 116° E	Tseng et al. (2007)
ESTOC site	1.55	1995–2004	29.16° N, 15.5° W	Santana-Casino et al. (2007)
BATS	1.67 ± 0.28	1983–2005	31.7° N, 64.5° W	Bates (2007)
UB	3.36 ± 0.22	1995–2004	36° N–38° N, 130° E–133° E	This study
Global Mean	1.5			IPCC (2007)
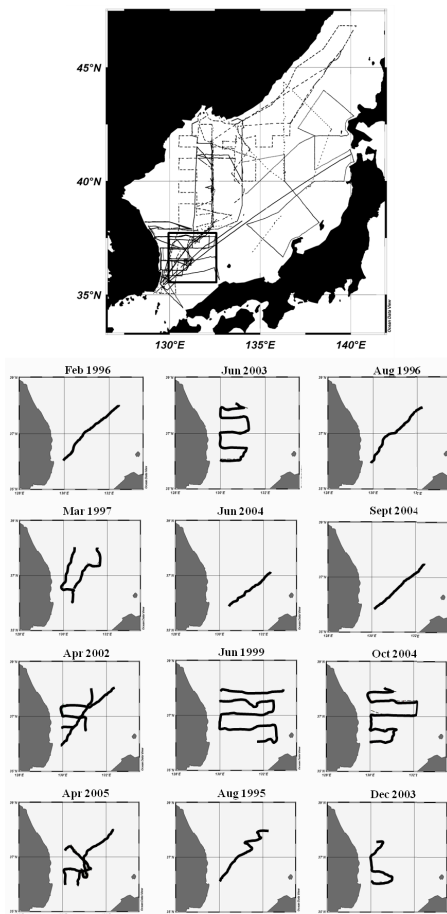
Fig. 1. Maps showing the tracks of the cruises conducted between 1995 and 2004 for this study.
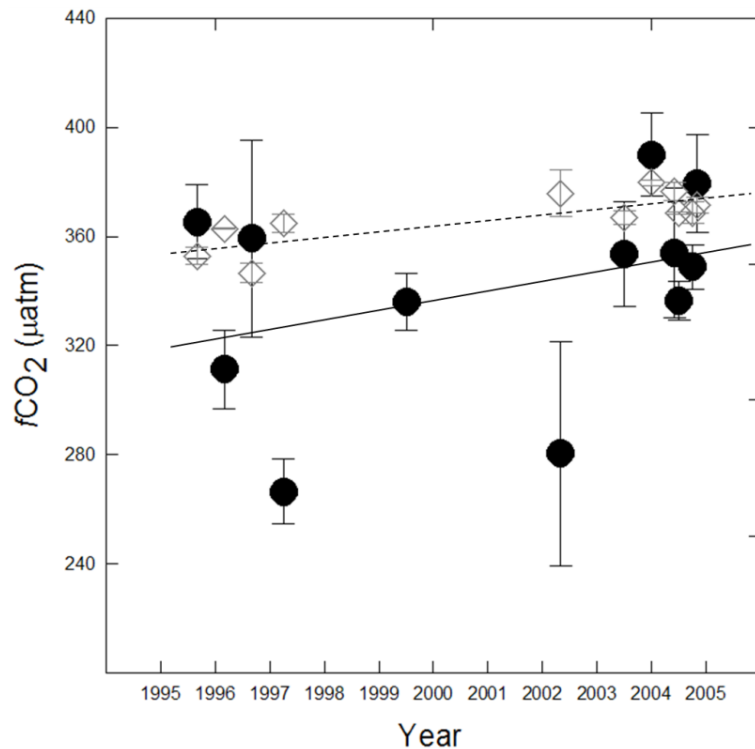
Fig. 2. The annual variations in $f\mathrm{CO}_2^{\mathrm{sea}}$ (filled circles) and $f\mathrm{CO}_2^{\mathrm{air}}$ (open diamonds) in the Ulleung Basin, East/Japan Sea, from 1995 to 2004. The slopes of the regression lines, which represent the annual increasing rate of $f\mathrm{CO}_2$ in the surface seawater (solid line) and in the atmosphere (dashed line) are $3.36\,\mu\mathrm{atm\,yr}^{-1}$ and $1.97\,\mu\mathrm{atm\,yr}^{-1}$, respectively. Error bars represent one standard deviation from the mean value.

Title Page

Abstract | Introduction

Conclusions | References

Tables | Figures

|◄ | ►|

◄ | ►

Back | Close

Full Screen / Esc

Printer-friendly Version

Interactive Discussion
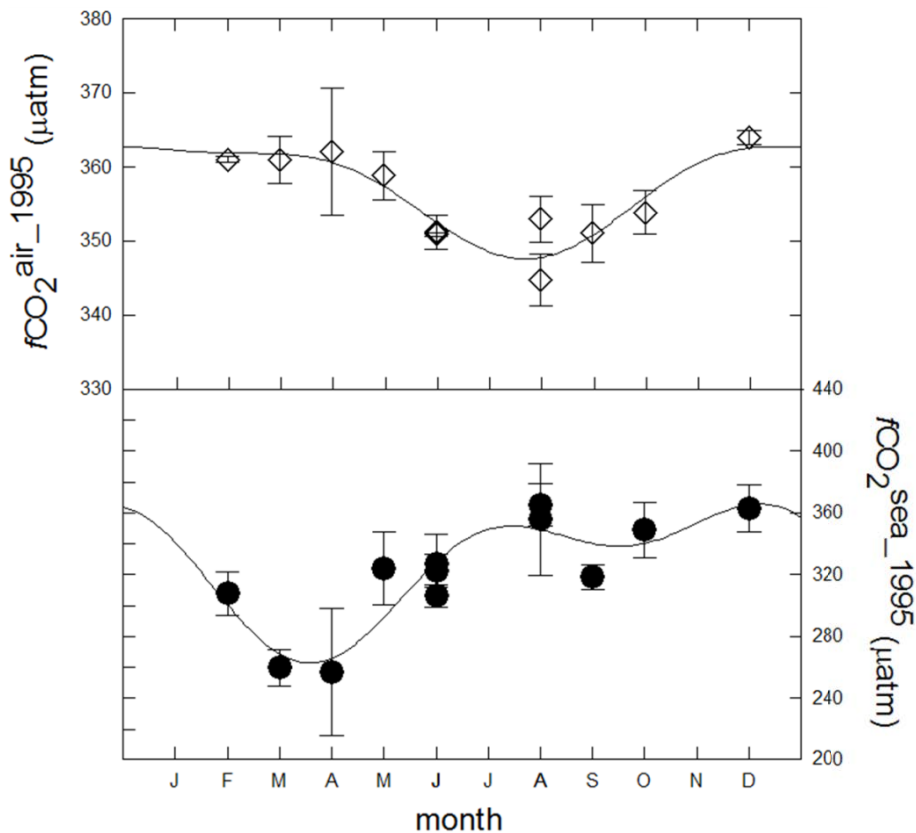
Fig. 3. Monthly variations in $f\mathrm{CO}_2^{\mathrm{air}}$ (open diamonds) and $f\mathrm{CO}_2^{\mathrm{sea}}$ (filled circles) normalized to the secular variation of the year 1995. The curves represent the results of harmonic function analysis.

Discussion Paper | Discussion Paper | Discussion Paper | Discussion Paper |

BGD

10, 9573–9602, 2013

Rapid increasing trend of CO₂ and ocean acidification

J.-Y. Kim et al.

Title Page

Abstract | Introduction

Conclusions | References

Tables | Figures

◄ | ►

◄ | ►

Back | Close

Full Screen / Esc

Printer-friendly Version

Interactive Discussion
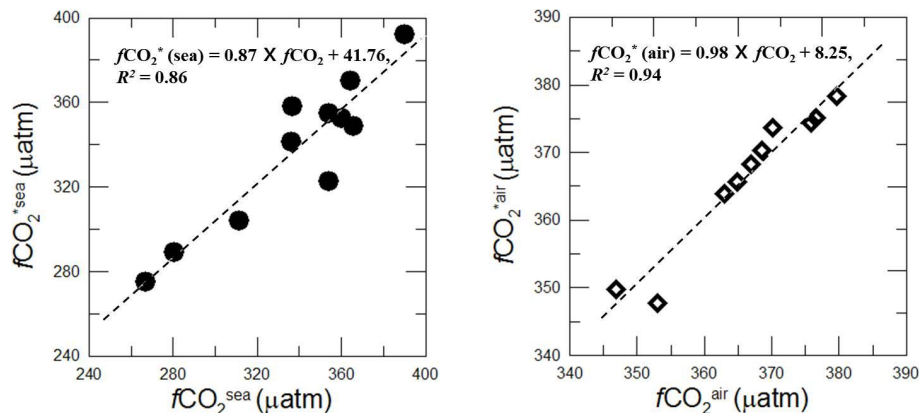
Fig. 4. Correlation between the fCO_2 and the fCO_2^* (estimated fCO_2) fitted from the harmonic function analysis. Filled circles denote fCO_2^{sea} and open diamonds did fCO_2^{air}, respectively. The root mean square deviations were estimated 13.6 µatm (sea) and 2.5 µatm (air), which were smaller than the standard deviation derived by the spatiotemporal averaging data of the UB (41.6 µatm in fCO_2^{sea} and 7.8 µatm in fCO_2^{air}).
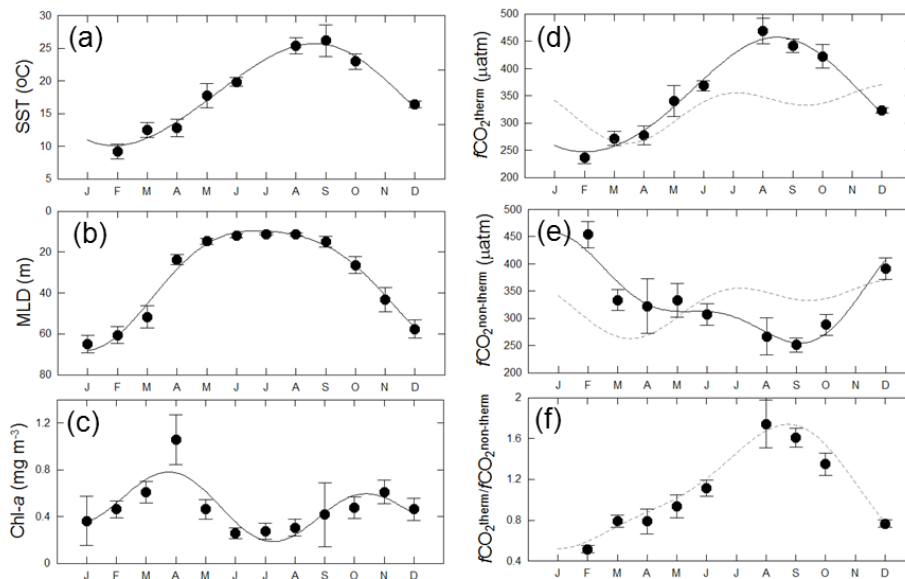
Fig. 5. Monthly variations in the **(a)** sea surface temperature (SST), **(b)** mixed layer depth (MLD), **(c)** chlorophyll a, **(d)** $f\mathrm{CO}_2^{\mathrm{therm}}$, **(e)** $f\mathrm{CO}_2^{\mathrm{non\text{-}therm}}$, and **(f)** ratio of the thermal to non-thermal effects ($f\mathrm{CO}_2^{\mathrm{therm}}/f\mathrm{CO}_2^{\mathrm{non\text{-}therm}}$) in the Ulleung Basin. The MLD was based on the climatology by de Boyer-Montegut et al. (2004). The chlorophyll a was based on the SeaWiFS data between 1998 to 2007. The $f\mathrm{CO}_2^{\mathrm{in\text{-}situ}}$ cycle (dashed line) was also shown in the (**d** and **e**) for the comparison with $f\mathrm{CO}_2^{\mathrm{therm}}$ and $f\mathrm{CO}_2^{\mathrm{non\text{-}therm}}$ variation.
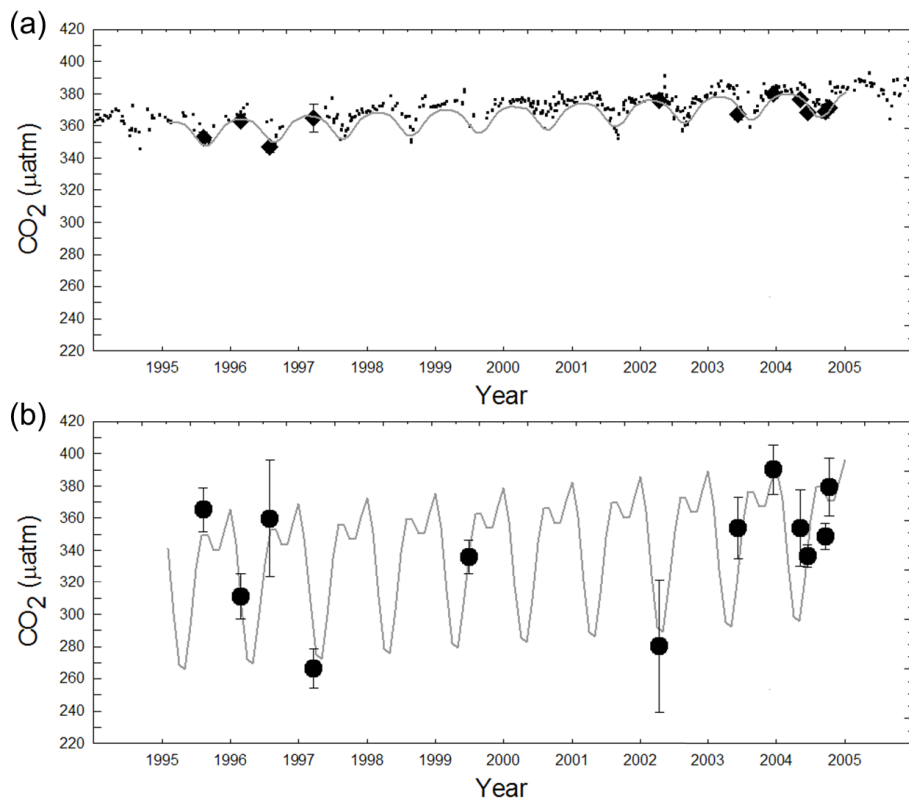
Fig. 6. Decadal trend of $f\text{CO}_2$ at the Ulleung Basin from 1995 to 2004. **(a)** $f\text{CO}_2^{\text{air}}$ (filled diamonds) of overlying atmosphere of the Ulleung Basin. Atmospheric $p\text{CO}_2$ data, measured at Gosan, Jeju Island, Korea (black dots), are also shown for comparison with $f\text{CO}_2^{\text{air}}$, **(b)** $f\text{CO}_2^{\text{sea}}$ (filled circles) of surface seawater of the Ulleung Basin. The gray curves represent $f\text{CO}_2^*$ modeled from a linear increasing trend and a harmonic function analysis (after Eq. 3).
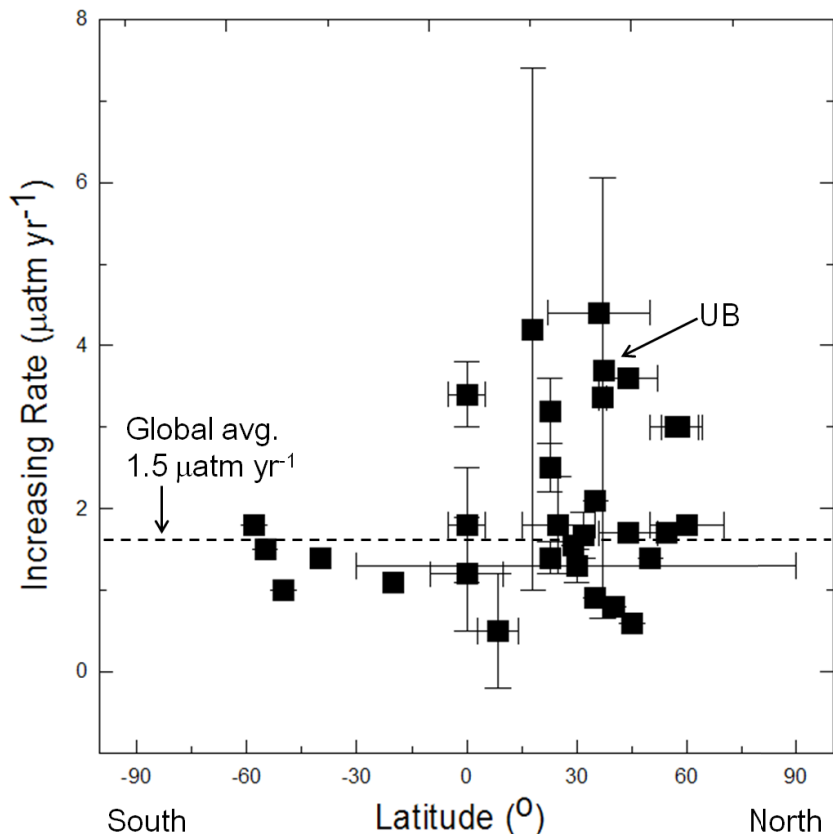
Fig. 7. A plot of the rate of increase of surface seawater CO_2 versus latitude. Dashed line represents the global average of surface seawater increasing rate ($1.5\,\mu atm\,yr^{-1}$).

Title Page

Abstract | Introduction

Conclusions | References

Tables | Figures

|◄ | ►|

◄ | ►

Back | Close

Full Screen / Esc
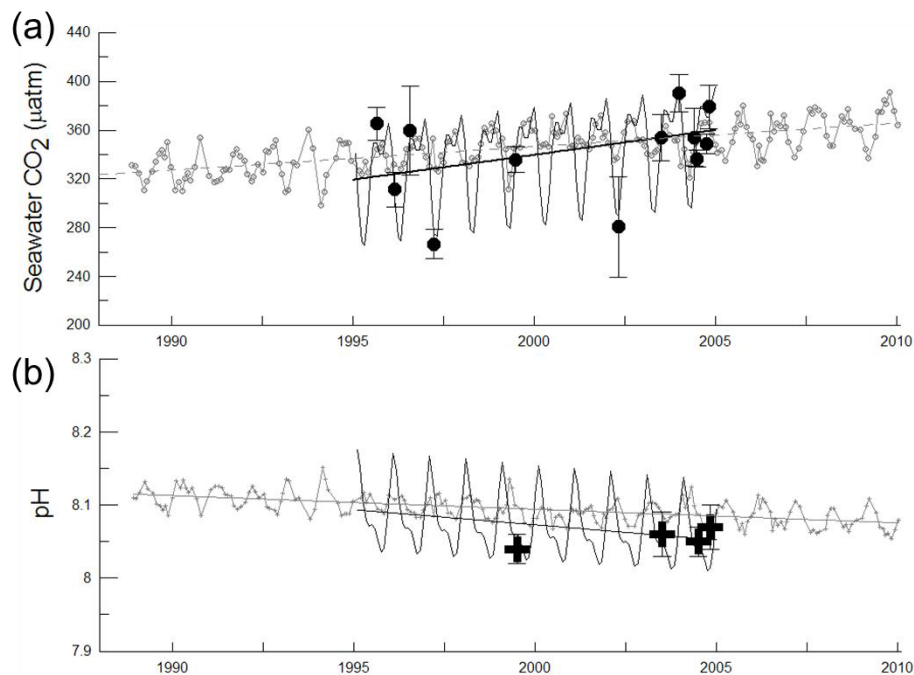
Printer-friendly Version

Interactive Discussion

Fig. 8. Secular variation in surface seawater **(a)** fCO$_2$ (µatm) (black filled circles and fitting line), and **(b)** pH (black crosses and fitting line) in the UB. The time-series pCO$_2$ (µatm) (gray open circles) and pH (gray dots) at Station ALOHA in the subtropical North Pacific Ocean are also shown for comparison. The pCO$_2$ and pH data at Station ALOHA are from David Karl, University of Hawaii, http://hahana.soest.hawaii.edu, and are updated from Doney et al. (2009) and Dore et al. (2003).